Journal of Applied Polymer Science

Improved impact strength of epoxy by the addition of functionalized multiwalled carbon nanotubes and reactive diluent

Wellington Marcos da Silva,[1] Hélio Ribeiro,[1] Juliana Cardoso Neves,[1] Alexandre Rangel Sousa,[2] Glaura Goulart Silva[1]

[1]Departamento de Química, Instituto de Ciências Exatas, Universidade Federal de Minas Gerais, Avenida Antônio Carlos, 6627, Belo Horizonte Minas Gerais, Brazil

[2]Centro Federal de Educação Tecnológica de Minas Gerais, Avenida Amazonas, 5253, Belo Horizonte Minas Gerais, Brazil

Correspondence to: G. G. Silva (E-mail: glaurag@qui.ufmg.br)

ABSTRACT: Multiwalled carbon nanotubes (MWCNTs), both oxidized and amine functionalized (triethylenetetramine—TETA), have been used to improve the mechanical properties of nanocomposites based on epoxy resin. The TGA and XPS analysis allowed the evaluation of the degree of chemical modification on MWCNTs. Nanocomposites were manufactured by a three-roll milling process with 0.1, 0.5, and 1.0 wt % of MWCNT–COOH and MWCNT–COTETA. A series of nanocomposites with 5.0 wt % of reactive diluent was also prepared. Tensile and impact tests were conducted to evaluate the effects of the nanofillers and diluent on the mechanical properties of the nanocomposites. The results showed higher gains (258% increase) in the impact strength for nanocomposites manufactured with aminated MWCNTs. Optical microscopy (OM), scanning electron microscopy (SEM), and transmission electron microscopy (TEM) were used to investigate the overall filler distribution, the dispersion of individual nanotubes, and the interface adhesion on the nanocomposites. © 2015 Wiley Periodicals, Inc. J. Appl. Polym. Sci. **2015**, *132*, 42587.

KEYWORDS: epoxy; grafting; mechanical properties; multiwalled carbon nanotubes; nanocomposites

Received 7 February 2015; accepted 2 June 2015

DOI: 10.1002/app.42587

INTRODUCTION

Historically, an important reference regarding the synthesis of carbon nanotubes (CNTs) is the work of Oberlin and co-workers.[1] However, the work of Iijima introduced CNTs as key materials in the field of nanotechnology.[2] Since then, many potential applications have been proposed for these materials, and their application in composite materials has recently gained increased attention.[3–5] The growing use of CNTs as reinforcements in nanocomposite materials manufacturing occurs due to the high values of electrical conductivity, as well as the better thermal and mechanical properties than those of other materials.[6–10] Although many advances have been achieved in the field of nanocomposites with CNTs, the most significant challenge remains associated with separation methods, chemical modification, and the dispersion of CNTs in the matrix.[11] Therefore, many studies have been performed to produce nanocomposite epoxy/CNTs for structural and functional applications. However, two decades after the work of Ajayan and co-workers, the potential application of CNTs as reinforcements in an epoxy matrix remains limited because of the difficulty in dispersing CNT bundles and the low interfacial interaction between CNTs and the matrix.[12] One strategy used to improve the chemical specificity and to increase their interaction with the matrix is the chemical modification of CNTs.[13,14] In the case of nanocomposites manufactured with epoxy resin and aminated CNTs, the amine groups present in the CNT structure improve the dispersion of the filler in the matrix due to the increased polarity.[15] Moreover, the reaction of amine groups with epoxy groups forming covalent bonds allows property enhancements.[16,17]

Particularly, the epoxy resins are thermosetting polymers used in the development of structural composites due to their high tensile strength, good chemical resistance, high adhesion, and low shrinkage.[18,19] However, the cross-linked resins are generally brittle materials with low fatigue resistance to heat and impact, which limits their application. CNTs can contribute to the improvement of mechanical and thermal properties, such as tensile strength, modulus of elasticity, impact resistance, and increase in the glass transition temperature in high-performance nanocomposites.[19,20] Guo and co-workers dispersed 2.0, 4.0, 6.0, and 8.0 wt % of oxidized MWCNTs directly in epoxy resin

Additional Supporting Information may be found in the online version of this article.

and observed that the tensile strength increased with the increasing wt % of MWCNTs.[21] Nanocomposites with concentrations between 0.1 and 2.0 wt % of MWCNTs and oxidized MWCNTs exhibited gains between 11 and 60% for tensile strength and between 23 and 57% for the elastic modulus.[22–26] For MWCNTs functionalized with triethylenetetramine (TETA), Cui and co-workers observed an increase of 50% in the tensile strength and 100% in the elastic modulus for the nanocomposites with 0.6 wt % MWCNTs.[27] Gains of 84 and 97.4% in the impact strength for the nanocomposite with the same concentration of the MWCNTs functionalized with TETA are described in the literature.[20,28] A maximum increase of 400% in the impact strength in polymeric nanocomposites consisting of various matrices and other nanofillers is described in the literature.[29,30]

Another strategy used to increase the impact resistance of nanocomposites is the addition of reactive diluents in epoxy systems. Chen and co-workers added 40.0 wt % of *n*-butyl glycidyl ether to epoxy resin (Bisphenol F) and achieved a 77.6% increase in the impact resistance.[31] Bakar and co-workers manufactured epoxy composites with kaolin and 2.5 wt % of phenyl diglycidyl ether and obtained an increase of 180% in the impact strength.[32] Moreover, Rahman and co-workers added 10.0 wt % of polyether polyol and 0.3 wt % of aminated MWCNTs to an epoxy system and observed gains of 18% in strength, 16% in modulus, and 99% in strain energy.[33] Yi and co-workers observed gains of 23.6% in the impact strength of nanocomposites manufactured with 15.0 wt % of oligomer and 0.5 wt % of CNTs oxidized in the epoxy matrix.[34] It is important to note that the properties of the cured composites are highly dependent on the structure of the cured network. After the addition of MWCNT and diluent, the network structure may change, which can impact the mechanical properties.[35]

In this study, MWCNTs were chemically modified using a microwave-based methodology and characterized with respect to chemical and morphological features. The CNT samples used for the composite preparation were well defined and of high quality and were tailored with surface functionalization to strongly interact with the epoxy. Nanocomposites were prepared with 0.1, 0.5, and 1.0 wt % of oxidized and aminated MWCNTs using the three-roll milling process. Tensile and impact tests were performed to evaluate the influence of the addition of oxidized and aminated MWCNTs, as well as the reactive diluent dipropylene glycol diglycidyl ether, on the mechanical properties of the nanocomposites. Microscopic images were used to evaluate the dispersion and morphology of the fracture surfaces of the nanocomposites. Higher values of impact strength, superior to those from similar studies in the literature, were found in the nanocomposites containing aminated MWCNTs. Furthermore, the presence of the diluent guarantees the maintenance of these high values of impact strength in the case of concentrated CNT samples.

EXPERIMENTAL

Materials

The MWCNTs ($C_{tube}100$) were purchased from CNT CO. LTD. in Korea. According to the manufacturer and as confirmed by thermogravimetric analysis (TGA), these nanotubes have a minimum purity of 93%. The supplier states that $C_{tube}100$ has an average diameter between 10 and 40 nm and a length between 1 and 25 μm. These data were confirmed by in-house measurements. DER 331 liquid epoxy resin (based on diglycidyl ether of bisphenol A—DGEBA), the curing agent DEH 24 (based on triethylenetetramine—TETA), and DER 736 liquid epoxy resin (based on dipropylene glycol diglycidyl ether-reactive diluent) were supplied by the DOW Chemical Company and were used as received.

Chemical Modification of MWCNTs

Initially, the MWCNTs were oxidized with a mixture of sulfuric acid/nitric acid (H_2SO_4/HNO_3, 3 : 1). The reaction mixture remained in a sonicator bath for 3 h. After oxidation, the mixture was centrifuged, filtered, and washed until the pH reached ~5.5–6.0. The filtrate was dried at 100°C for 12 h and named MWCNT–COOH. For functionalization, 70 mL of TETA was added to 6 g of MWCNT–COOH. The bottle containing the reaction mixture was connected to the microwave reactor, which operated between 80 and 120°C with an increasing power of 0–140 W, adjusted by increments of 10 W every 40 min.[36,37] Subsequently, the mixture was cooled, dispersed in 300 mL of anhydrous ethanol, and then filtered and washed to remove the TETA adsorbed on the tube walls. The filtered material was dried in an oven at 100°C for 12 h and named MWCNT–COTETA.

Preparation of Nanocomposites

Initially, a study was conducted by DSC to determine the best resin/hardener ratio according to the work of Garcia and co-workers.[38] The results and discussion related to this study are presented as Supplementary Information (SI). Then, nanocomposites were prepared with concentrations of 0.1, 0.5, and 1.0 wt % of MWCNT–COOH and MWCNT–COTETA with 0.0 and 5.0 wt % of diluent. Two stages of dispersion were performed. In the first step, MWCNTs were dispersed in the matrix (epoxy resin or epoxy resin plus diluent) for 30 min using a mechanical stirrer operating at 2400 rpm and 80°C. In the second step, a three-roll mill was used to improve the dispersion. In this case, the predispersion passed three times through the rollers, which were located at a distance of 5 μm, with a temperature of 80°C and a velocity of 250 rpm. Subsequently, the dispersion was degassed under vacuum at 80°C and under magnetic stirring for 2 h. The dispersion was cooled, and the mass of the hardener, corresponding to 14.8 phr (parts by weight of curing agent in one hundred parts of resin), was added to the dispersion, which was agitated slowly and transferred to silicone molds. The addition of 5.0 wt % of diluent changes the epoxy/TETA ratio. Therefore, calculations were performed to consider the diluent, and the new formulation for the TETA concentration is 14.82 phr (14.82 parts of TETA per 100 parts of epoxy resin). The curing was performed in two steps: initially, at room temperature for 24 h and then at 135°C for 4 h. The addition of 5 wt % of the diluent decreases the viscosity of the epoxy system almost one order of magnitude (from 12 to 4.4×10^3 cP at 25°C), which can be beneficial to improve the dispersion of CNTs in the epoxy matrix.

Characterization

Thermogravimetric analysis (TGA) was performed using a TGA Q5000 from TA Instruments. The samples were analyzed from 30 to 1000°C at a heating rate of 5°C·min^{-1} under a synthetic airflow of 70 mL·min^{-1}.

The X-ray photoelectron spectroscopy (XPS) spectra were obtained at room temperature on a VG Scientific Escalab 220-ixL system. The base pressure in the vacuum chamber was 2.0 $\times$ 10^{-10} mbar using an Mg anode to generate X-rays on the K_α line ($E = 1487$ eV). Stretched XPS spectra between 0 and 1000 eV were obtained with 1-eV steps. A high-resolution spectrum with 0.1-eV steps was obtained in the peak region of photoemission for C 1s, N 1s, and O 1s electrons. The electron energy analyzer was operated in the large-area mode ($\varnothing = 4$ mm) with a pass energy of 50 eV for stretched spectra and 20 eV for the analysis of individual lines. Each spectrum was adjusted using a combination of Gaussian and Lorentzian functions.

Optical microscopy (OM) images were obtained with transmitted light and 20× magnification on an Olympus BX50 microscope fitted with a digital camera Olympus C-7070. The samples were prepared by depositing one drop of the nanocomposite dispersion (before curing) between two coverslips.

Scanning electron microscopy (SEM) images were obtained with a Quanta 200 model FEG-FEI 2006 microscope operating under vacuum with a 30.0 kV accelerating voltage. Using conductive carbon tape, the fractured samples were fixed in the sample holder. The samples of the neat epoxy and nanocomposites were exposed to a cloud of sublimed gold to achieve coating with a metal layer that was approximately 15 nm thick. To obtain the images of the MWCNTs, the equipment was operated in STEM mode, and the samples were dispersed in propanol for 5 min using an ultrasonic bath. After the dispersion, one drop was placed onto a 200-mesh holey carbon copper grid.

Transmission electron microscopy (TEM) micrographs were obtained on an FEI TECNAI G2 microscope with a 200 kV tungsten filament. Using an ultramicrotome (Laika model UC6), 40-nm-thick nanocomposite slices were cut with a diamond blade under the following conditions: temperature between 20 and 22°C and a shear rate of 3 mm s^{-1}. The slices were deposited onto a copper grid with 200-mesh openings.

Tensile-strength tests were performed on a Shimadzu model SPL autograph AGX with a maximum capacity of 10 kN, as asserted by ASTM D 638-03 under the following conditions: average temperature of 23°C and relative humidity of 57%. Eight samples were prepared with standard dimensions of the model corresponding to the specimen TYPE I.

Izod impact tests were performed according to ASTM D 256-10 (method A) on an XJ series impact-testing machine, model XJ-25Z under the following conditions: average temperature of 24°C and relative humidity of 55%. In tests of 1.0 J, a hammer with an impact speed of 3.5 m/s was used. Five samples were prepared with standard dimensions of average width (10.4 $\pm$ 0.2) mm.

RESULTS AND DISCUSSION

Thermal Properties and Morphology of the Nanofillers

Figure 1(a,b) presents the curves corresponding to the mass loss as a function of temperature and the derivative of the TGA curve (DTG) for the neat and modified carbon nanotubes prepared in this work. The thermograms in Figure 1(a) show only one stage of decomposition for the MWCNT sample at temperatures between 450 and 650°C, which is a typical result for MWCNTs.[39] For the chemically modified samples, the mass loss occurs below 400°C and at variable temperatures due to the various functional groups placed on the tube surface.[14,40–42] The DTG curves (Figure 1b) allow the identification of an initial weight loss at 100°C associated with humidity (1.5 and 1.8%) in the chemically modified samples. For the sample of MWCNT–COOH, the event at 160°C is associated with the decomposition of the various oxygenated groups (7%). The event observed at 290°C for the MWCNT–COTETA sample (16%) can be associated with the decomposition of the TETA-based groups and residual oxygenated groups that did not react with TETA. These groups were identified by XPS analysis. The principal event, which was the nanotube decomposition at approximately 600°C, shows differences between the modified and unmodified MWCNTs; in the latter, the decomposition occurs over a lower range of temperatures.

The STEM image [Figure 1(c–e)] shows that certain MWCNTs are more than 2 μm in length and that the small tubes are arranged in bundles, indicating that the chemical modification steps did not reduce the size of the CNTs. The presence of impurities does not appear in the images, which is corroborated by the TGA analysis.

XPS Spectra

XPS spectra were obtained in the regions of the primary elements of interest (C, O, and N). Figure 2 shows the XPS survey spectra of the MWCNT, MWCNT–COOH, and MWCNT–COTETA samples.

All the samples show photoemission peaks for C 1s (285.0 eV).[27] The O 1s (532.0 eV) and N 1s (400.0 eV) peaks are only observed in the spectra of the chemically modified samples.

Figure 3 shows the high-resolution photoemission spectra of the signals for each chemical species and the lines associated with various contributions, which were obtained through adjustments with the combined Gaussian and Lorentzian functions. The photoemission C 1s peaks were studied between 280.0 and 294.0 eV. Figure 3(a–c) shows a dominant peak at 284.5 eV, assigned to the sp^2-hybridized C—C bonds in extensive π-conjugated systems.[43] A secondary peak is verified at 285.5 eV, which is characteristic of sp^3-hybridized C—C bonds present at defective locations and the tubular structure asymmetry. Two additional photoemission peaks are observed at 286.5 and 287.2 eV [Figure 3(c and b), respectively]. The first peak is attributed to carbon atoms bonded to oxygen atoms (—C—O—R), and the second peak is characteristic of carbon atoms pertaining to carbonyl groups (—C═O).[44] At 291.0 eV [Figure 3(b)], a satellite peak is observed, which is caused by the π-–π^* electronic transition corresponding to the photoemission peak at 284.5 eV, which arises due to the presence of photoelectrons that have

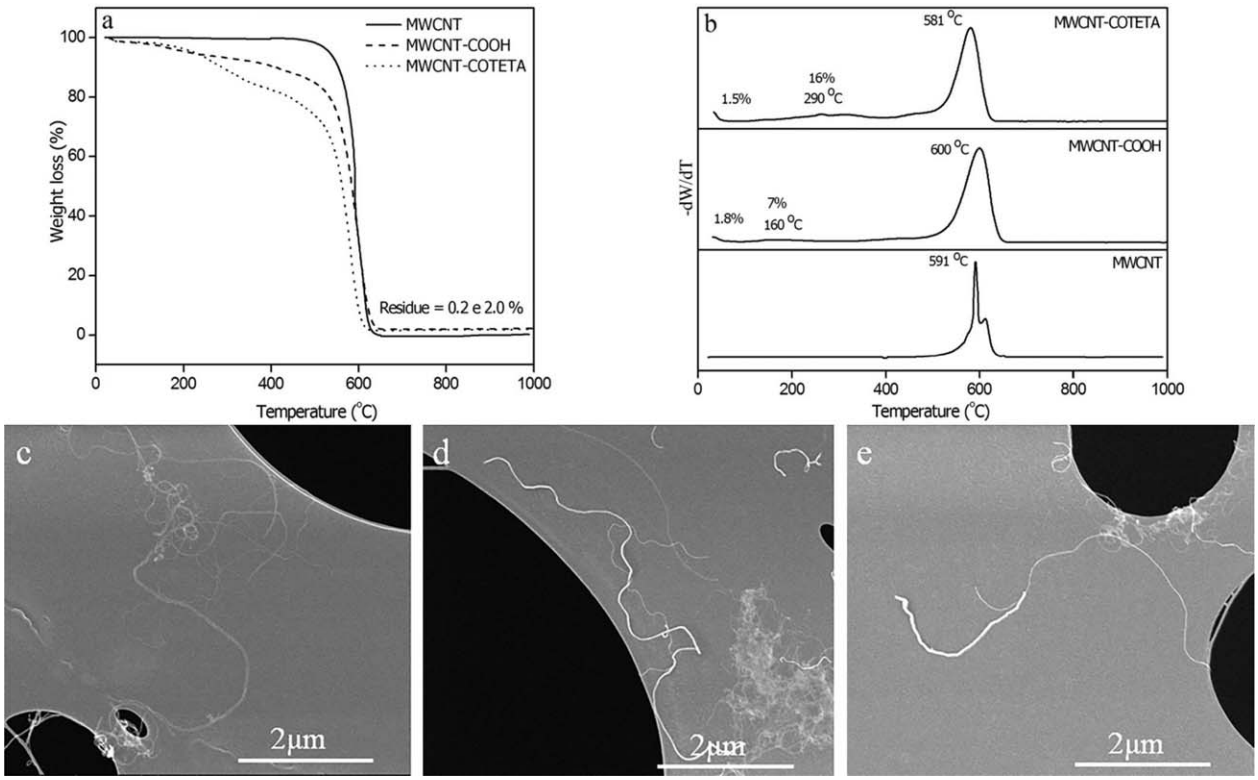

Figure 1. (a) TG and (b) DTG curves for MWCNT, MWCNT–COOH, and MWCNT–COTETA samples; STEM images for (c) MWCNT, (d) MWCNT–COOH, and (e) MWCNT–COTETA.

lost their kinetic energy in this transition, indicating the existence of a high degree of electron delocalization.[28,45] Evidence of the presence of carboxylic groups is determined by the observation of a peak at 288.6 eV [Figure 3(b)], which is typical for this functional group.[44] Figure 3(c) shows the presence of carbon of the —N—C═O bond with absorption at 287.6 eV. This observation of carbon in the amide group shows the efficiency of the covalent functionalization of MWCNTs with TETA.

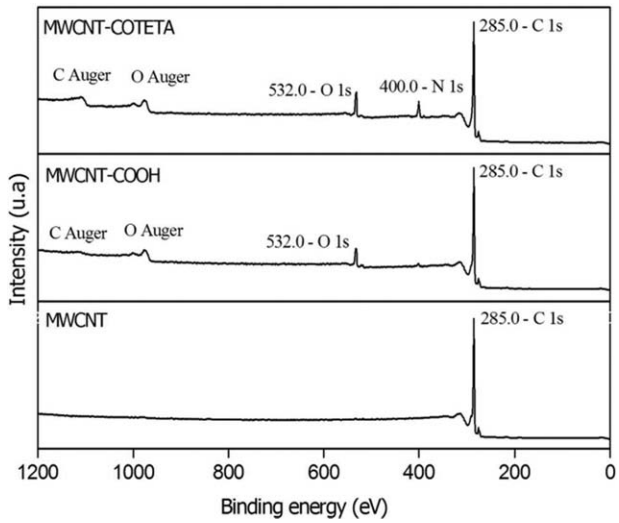

Figure 2. XPS survey spectra for the MWCNT, MWCNT–COOH, and MWCNT–COTETA samples.

Oxidation and functionalization peaks associated with the C—O and C═O bonds at 532.1 and 533.5 eV, respectively, were also observed [Figure 3(d,e), respectively].[28] Following the functionalization with TETA, the reduction of the carbonyl moiety of the carboxylic acid groups [Figure 3(e)] with amide formation is noted. The presence of an amide carbonyl appears in the spectrum of N 1s [Figure 3(f)], as well as in the XPS spectra in the C and O regions, as previously discussed. After adjustments of the photoemission peaks, three significant contributions with bonding energies from 400.2–402.3 eV were identified. Nitrogen atoms with a bonding energy of 400.2 eV are present in bonds involving primary amines (—CH_2—NH_2). Nitrogen atoms with bonding energies at 401.0 eV are only bonded to amide carbonyl groups (—N—C═O), and those with bonding energies at 402.3 eV are bonded to secondary amines (—CH_2—NH—CH_2).[11,42,46] These results show that the TETA compound formed covalent bonds with the oxygenated groups on the nanotube surface, enabling the formation of primary bonds between the reinforcing filler nanotube and the epoxy matrix.

Mechanical Properties

Tensile and impact tests were performed to evaluate the effects of adding 5.0 wt % of diluent on the mechanical properties of MWCNT–COOH and MWCNT–COTETA-reinforced epoxy composites at three different concentrations. As shown in Figure 4, the addition of 0.1, 0.5, and 1.0 wt % of MWCNT–COOH and MWCNT–COTETA on the epoxy matrix led, in general, to a decrease in the values of tensile strength [Figure 4(a,b)] and ultimate strain [Figure 4(c,d)].

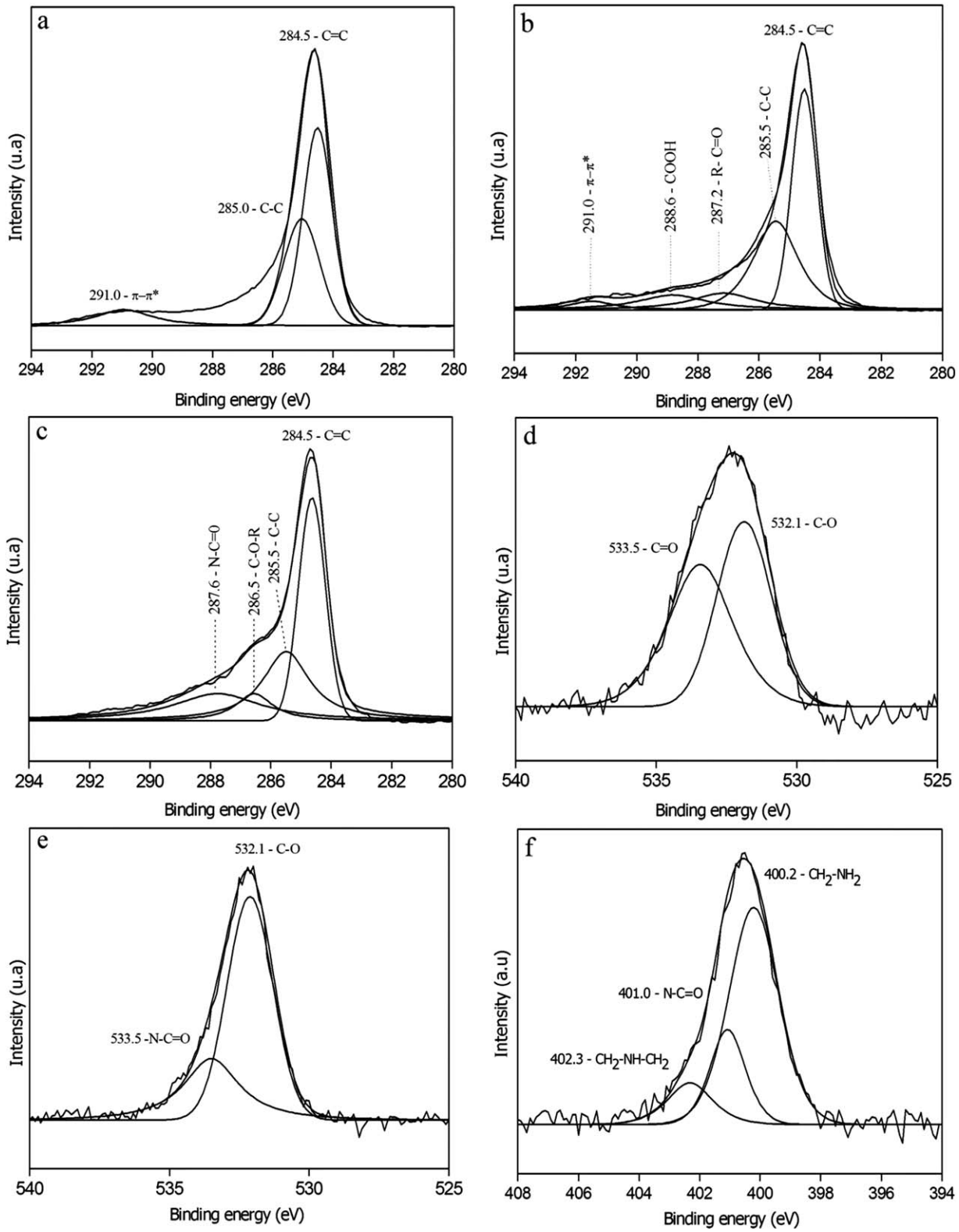

Figure 3. High-resolution XPS spectra obtained in the C 1s bonding energy region for (a) MWCNT, (b) MWCNT–COOH, and (c) MWCNT–COTETA samples. Signals for O 1s in (d) MWCNT–COOH, (e) MWCNT–COTETA, and (f) signals for N 1s of MWCNT–COTETA.

The tensile strength values of epoxy with 0.0 and 5.0 wt % of DER 736 were determined to be 46.1 and 54.6 MPa, respectively. For a concentration of 0.1 wt % of nanotubes, independent of the type of reinforcing filler surface modification, the nanocomposite performances for the tensile strength and ultimate strain were similar to those observed with the non-reinforced epoxy.

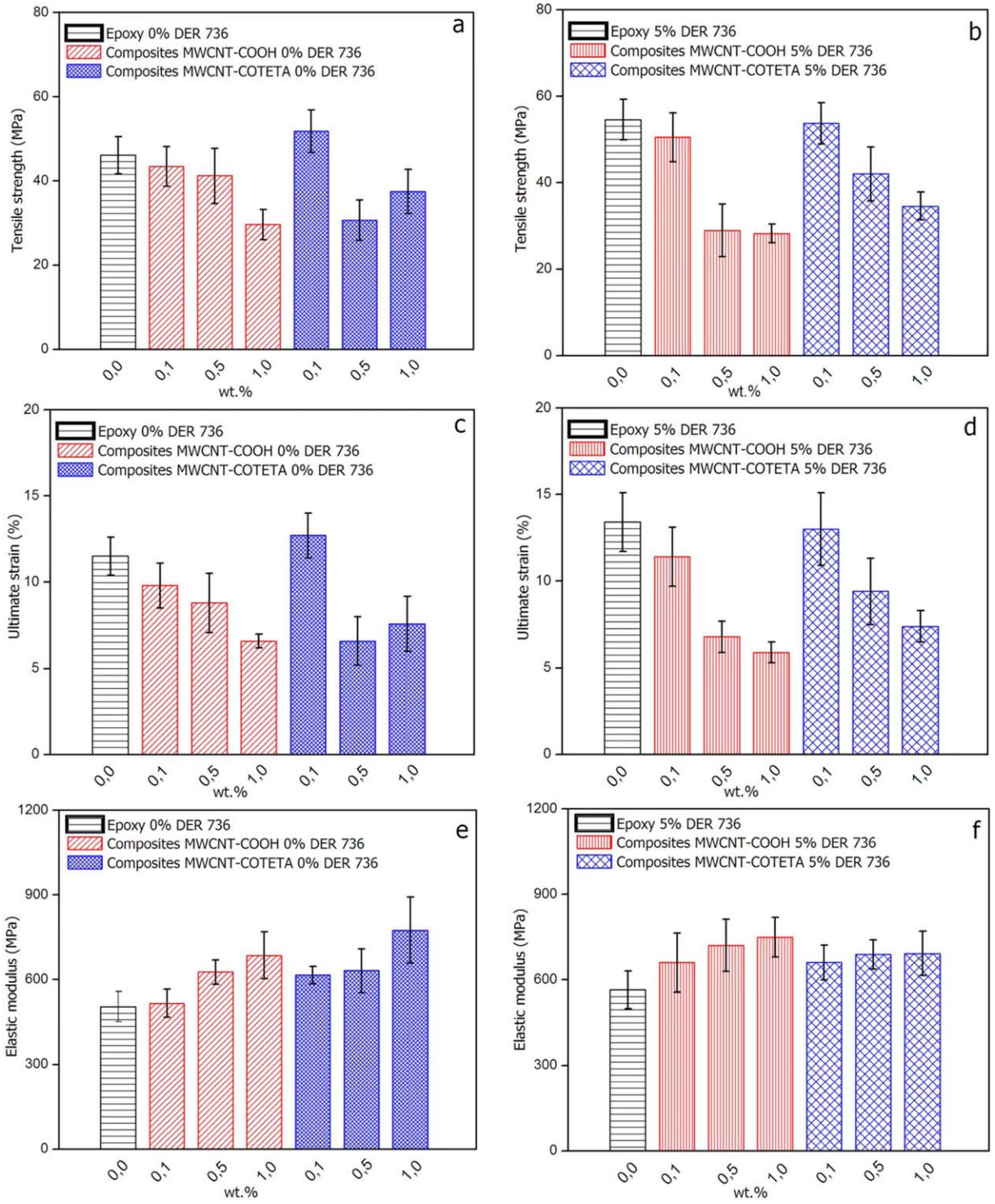

Figure 4. Mechanical properties vs wt % of MWCNT–COOH and MWCNT–COTETA (a, c, e) with 0.0 wt % and (b, d, f) with 5.0 wt % of diluent. [Color figure can be viewed in the online issue, which is available at wileyonlinelibrary.com.]

A possible explanation for the decrease in the values of the tensile strength and ultimate strain observed in Figure 4 is that the reduction is related either to the high degree of stiffness of the MWCNTs, resulting in the failure of the nanocomposites, or to the increase in the agglomerate size with the wt % of MWCNTs, as observed in Figure 5.[47–49] The agglomerates can act to increase the stress, which facilitates the initiation of cracks. The small agglomerates are related to the preparation process of nanocomposites; in this case, the separation of 5 μm between the rolls in the three-roll milling allows the disaggregation of

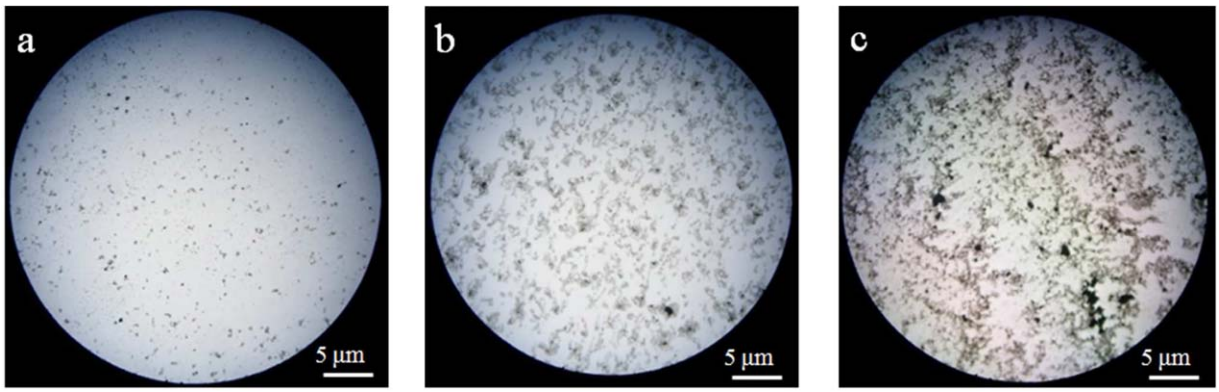

Figure 5. OM images of the nanocomposites for (a) 0.1; (b) 0.5; and (c) 1.0 wt % of MWCNT–COOH with 0.0 wt % of diluent. [Color figure can be viewed in the online issue, which is available at wileyonlinelibrary.com.]

agglomerates of larger dimensions, exerting a strong shear stress on MWCNTs but without causing excessive breaks of the individual MWCNTs.[50,51] For the MWCNT–COOH samples, the OM images in Figure 5 showed that micron-scale aggregates are present in all nanocomposites with a homogeneous distribution across the sample, but large regions with gray tone also exist. This is also the case for the MWCNT–COTETA-based nanocomposites. In the gray regions, there are isolated tubes and nanoaggregates, which will be discussed later based on SEM and TEM images.

The results of the tensile tests for the elastic modulus are presented in Figure 4(e) and (f), which are the inverse of those observed for the tensile strength and ultimate strain. The results show that for a larger amount of filler, the elastic modulus values increase. An increase in the elastic modulus is common with the increasing wt % of CNTs and other nanofillers.[27,48,52] The MWCNT–COTETA was more efficient in terms of improvement in the elastic modulus, proving the relevance of surface functionalization.[26] Amino groups located on the CNT surface will react to form covalent bonds with the epoxy, resulting in significantly enhanced interfacial adhesion. The results show an increase in the elastic modulus of 53.5% for the nanocomposite containing 1.0 wt % relative to the epoxy with 0.0 wt % of diluent. The addition of diluent to the nanocomposites resulted in similar gains in the elastic modulus with respect to the system without diluent, except for the case of the 1.0 wt % MWCNT–COTETA composite.

Figure 6 shows the behavior of the epoxy system and the nanocomposites with 0.0 and 5.0 wt % of diluent and with the various fillers when subjected to the Izod impact tests.

Figure 6 shows that the values of the impact strength for the nanocomposites are in general greater than those of the epoxy systems, except for those for nanocomposites with 0.5 and 1.0 wt % of MWCNT–COOH without diluent [Figure 6(a)] and with 1.0 wt % of MWCNT–COOH and 5.0 wt % of diluent [Figure 6(b)], considering the values of the uncertainties. An

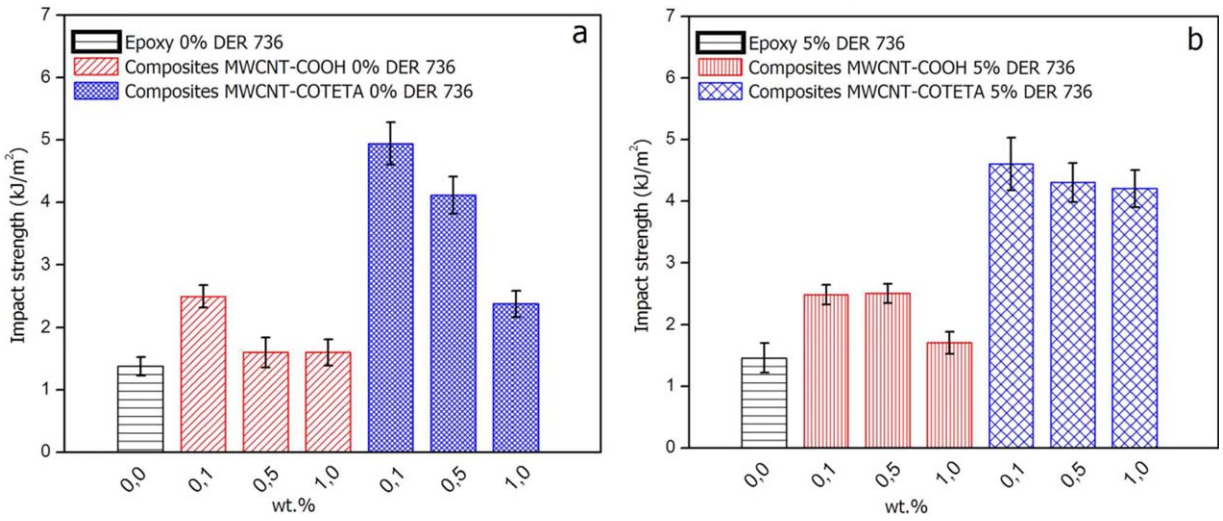

Figure 6. Impact strength vs wt % for MWCNT–COOH and MWCNT–COTETA with (a) 0.0 wt % and (b) 5.0 wt % of diluent. [Color figure can be viewed in the online issue, which is available at wileyonlinelibrary.com.]

observed trend is the progressive decrease in the values of the impact strength with increasing wt % of MWCNTs. This behavior was also observed in studies by other authors.[52–54] The composition range selected for this study was based on previous results from other groups[20,28,30] and from ourselves.[19] It would be interesting to study a less concentrated sample (e.g., 0.05 wt %) in the case of the impact strength, although the elastic modulus results in Figure 4 indicate that more concentrated samples would also be of interest. Therefore, considering the various parameters already being exploited in this work, the study was limited to three concentrations of composites.

Compared with the epoxy systems, higher gains are observed for the nanocomposite containing 0.1 wt % of MWCNT–COOH (81%) and MWCNT–COTETA (258 and 215%) with 0.0–5.0 wt % of diluent. The high values for the impact strength may be related to the functionalization of MWCNT–COTETA, which in this case can be attributed to the covalent bonds between the amine groups present in the MWCNT–COTETA and the epoxy groups present in the resin, as well as the direction of force applied to the test.[15] According to Yang and co-workers, TETA molecules covalently linked to an epoxy system increase the mobility of the polymer chains, favoring the load transfer between the MWCNTs and the resin, which leads to a high-impact energy absorption.[28] As described in the literature, gains higher than 400% of the impact strength values of polymeric nanocomposites were observed for systems consisting of multiple matrices and other nanofillers.[29,30] However, for nanocomposites prepared with epoxy resin and MWCNTs functionalized with TETA, the maximum increase observed was 97.4%.[20] Jajam and co-workers observed a toughness increase when adding diluent to an epoxy/CNT system subjected to impact tests. The initiation of the crack required a significantly longer time, and the crack speed propagation was reduced.[55]

Another interesting comparison can be made between the two composites with MWCNT–COTETA at 1.0 wt %. The system with diluent was able to maintain a higher value of impact strength with respect to the material without diluent addition. This behavior can be attributed to better dispersion of the nanofiller with the help of the lower viscosity of the material with diluent.

From the results of the mechanical tests, we observed that the presence of the CNTs effectively reinforces the epoxy resin, increasing its rigidity, as verified by the elastic modulus, and the impact resistance; the latter was particularly observed with CNT formulations modified with amine and diluent. The presence of the amine on the surface of the nanotube favors the load transfer from the matrix to the filler with the diluent, improving the dissipative characteristics; thus, these two combined features increase the impact resistance. However, these factors should also provide superior mechanical performance for the nanocomposite tensile strength compared with that of the pure resin, which was not observed. The tensile failure occurs from a stress concentrator, associated with clusters due to limited CNT dispersion. Moreover, the stress and the elongation at break decreased with an increasing concentration of the CNTs. The elasticity modulus exhibited gains with carbon nanotube addition because the elasticity modulus is not a property related to the break, therefore, reflecting the increase in the charge/matrix interactions. As for impact, the notch induces the starting point of failure, which reduces the action of the stress concentrators; thus, the property gains are significant. Furthermore, for all the compositions, the impact strength was higher than that of the neat resins. The greatest benefit was observed with the combination of amine-modified MWCNTs in the presence of the diluent, resulting in a good combination of increased load transfer from the matrix due to the reinforcement and dissipative effect caused by the diluent.

Morphology of the Fracture Surface

SEM images from the fracture surface of the impact samples were used to evaluate the interaction and the morphology of the epoxy and the nanocomposites (Figure 7). The images are representative of a series of images with the same profile. The fracture surface of epoxy with 0.0 wt % of diluent [Figure 7(a)] is smooth with continuous lines and spreading cracks, indicating typical behavior of brittle materials.[56] However, the epoxy with 5.0 wt % of diluent has a rough surface, indicating a tougher fracture.[55] Although increases in the tensile strength (18.4%) and ultimate strain (16.5%) occur in epoxy with 5.0 wt % of diluent relative to the epoxy with 0.0 wt %, the same tendency is observed in these two parameters with increases in the wt % of CNTs; thus, in both the systems, the fracture surface became rougher after the introduction of the CNTs. Figure 7(b) shows the presence of a few clusters on the fracture surface of 0.1 wt % MWCNT–COOH with 0.0 wt % of diluent. The clusters in the nanocomposites lead to stress concentration during the tensile tests, decreasing the tensile strength and the ultimate strain, which can explain the lower values found for the nanocomposites compared with that of epoxy with 0.0 wt % of diluent.[50]

Figure 7(c,d) indicates that there are strong interfacial interactions between the CNTs and epoxy in the composites. The tendency for short and curved patterns of crack propagation into the nanocomposites can be observed. When the crack propagates in nanocomposites through a nanotube, crack tips cannot break the strong MWCNTs due to bridging by cross-linking. Therefore, the crack tips are forced to arrest or change their crack propagation direction, resulting in a higher energy-absorption capability.[33,55]

Filler Distribution in the Epoxy Matrix

TEM images for the nanocomposites containing 0.1, 0.5, and 1.0 wt % of MWCNT–COOH and MWCNT–COTETA manufactured with 5.0 wt % of diluent are shown in Figure 8. Note that in all the images, there is a good dispersion of the CNTs in the matrix, and the density of the tubes in the aggregates increases with increasing wt % CNTs [Figure 8(b, c, and f)]. Although the OM images, such as those in Figure 5, showed that micron-scale aggregates are distributed in all samples, the TEM images indicated that the dispersion of MWCNT–COTETA in the matrix is better than that of MWCNT–COOH [Figure 8(d–f)].[15] This result is due to two different effects: first, the increased polarity of the mixture where the amino groups act as a Lewis base, reducing the interaction between

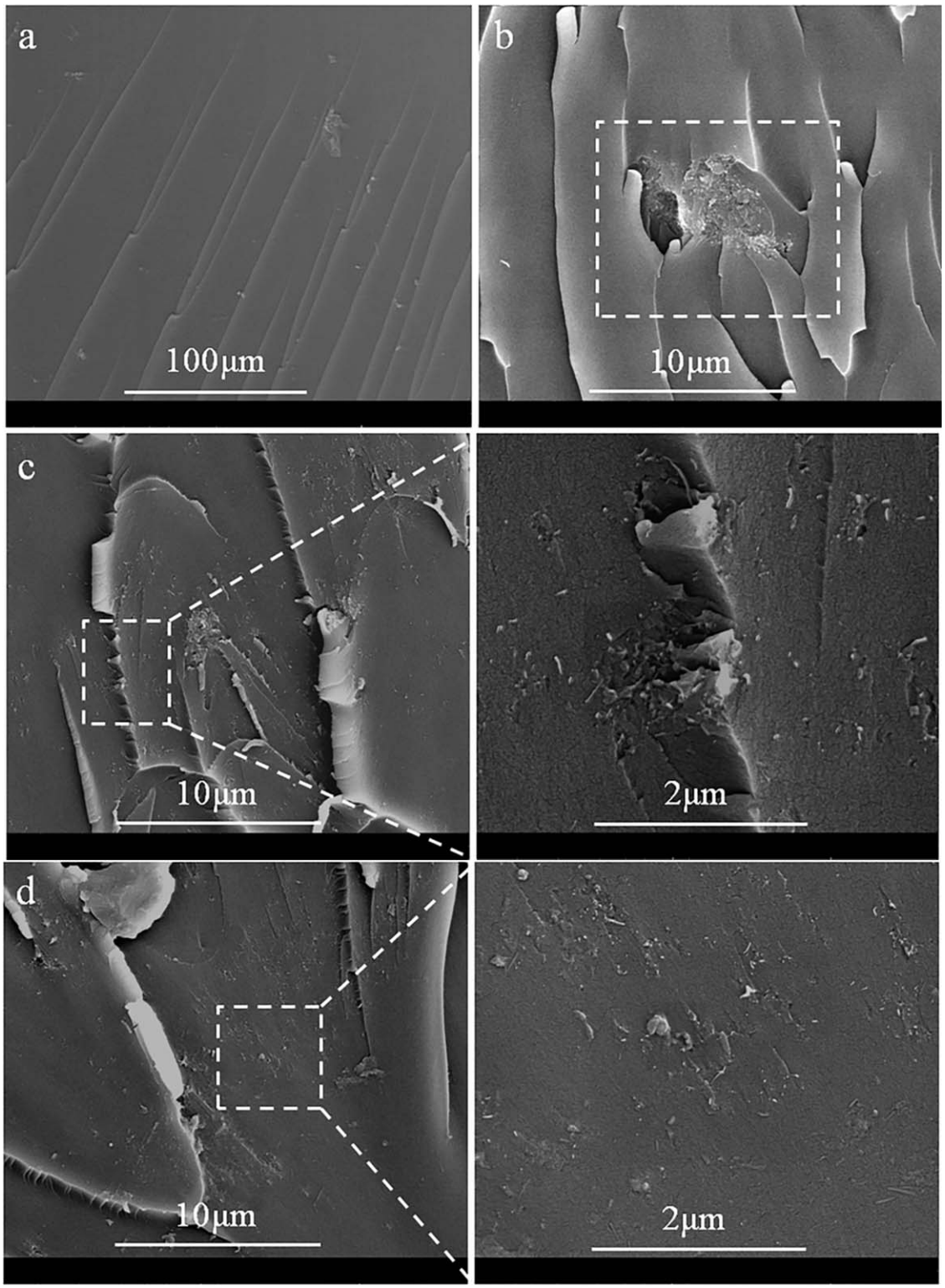

Figure 7. SEM images of fracture surfaces for (a) epoxy with 0.0 wt % of diluent; nanocomposites with (b) 0.1 wt % of MWCNT–COOH and 0.0 wt % of diluent; (c) 0.1 wt % of MWCNT–COTETA and 0.0 wt % of diluent; and (d) 0.1 wt % of MWCNT–COTETA with 5.0 wt % of diluent.

tubes and, thus, stabilizing the dispersion through interaction with the epoxy matrix. The second effect is a result of the covalent bonds between the amines and epoxy groups. These covalent bonds reduce aggregation that would occur during the cross-linking step. The strong adhesion of tubes to the matrix associated with the fracture mechanism may have contributed to the increase in the impact strength of the nanocomposites containing MWCNT–COTETA.

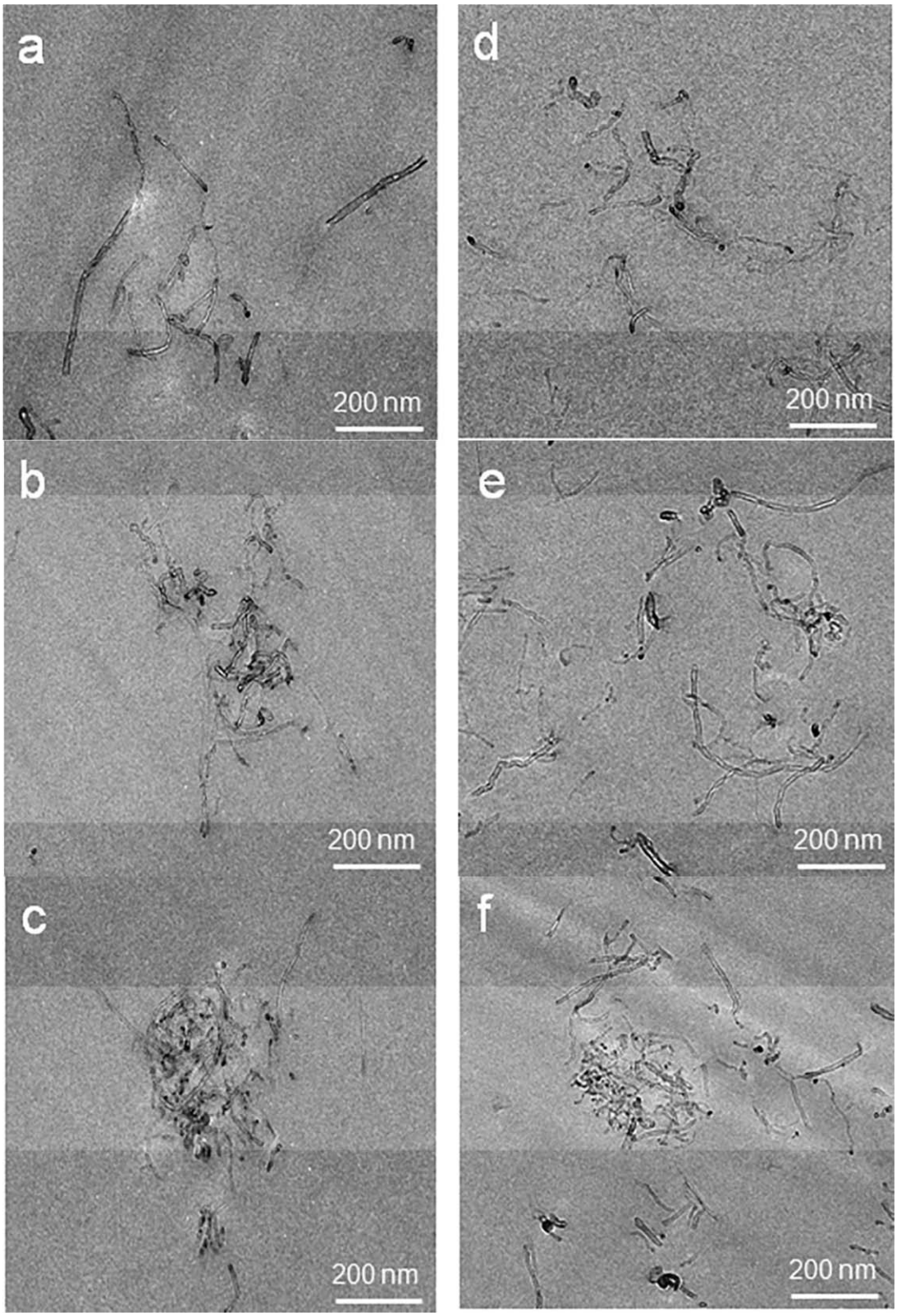

Figure 8. TEM images of the cryomicrotomed films (thickness of 40 nm) for the nanocomposites with 5.0 wt % of diluent for (a) 0.1 wt % of MWCNT–COOH, (b) 0.5 wt % of MWCNT–COOH, (c) 1.0 wt % of MWCNT–COOH, (d) 0.1 wt % of MWCNT–COTETA, (e) 0.5 wt % of MWCNT–COTETA, and (f) 1.0 wt % of MWCNT–COTETA.

CONCLUSIONS

In this study, oxidized and amine-functionalized MWCNTs were used to improve the mechanical properties of nanocomposites based on epoxy resin. An efficient route for chemical modification was used to covalently link the TETA molecule to the structure of the oxidized MWCNTs. The results of TGA/DTG indicate that 7 wt % of oxygenated functional groups were introduced by the acid treatment, and 16 wt % of the COTETA functional groups and other oxygenated functional groups decomposed at approximately 290°C. The XPS peaks between 400.2 and 402.3 eV indicate the presence of nitrogen functional groups in the structure of the MWCNT–COTETA. Nanocomposites containing 0.1, 0.5, and 1.0 wt % of MWCNT–COOH and MWCNT–COTETA with 0.0 and 5.0 wt % of diluent were produced by mechanical stirring and by three-roll milling. The results of the tensile and impact tests showed gains between 2 and 53% in the elastic modulus and between 16 and 258% in impact strength for nanocomposites manufactured with MWCNT–COOH and MWCNT–COTETA with or without diluent. The OM images show the presence of small clusters, which became more constant with an increase of the wt % of CNTs. Similarly, these clusters were also observed in the SEM images. The clusters in the nanocomposites lead to stress concentration during the tensile tests, decreasing the tensile strength and the ultimate strain, which can explain the lower values found for the nanocomposites compared with that of epoxy with 0.0 wt % of diluent. Additionally, as observed in the SEM images, the increase of roughness in the fracture surface is related to the increase in absorption of impact energy. From the analysis of these results, we can conclude that the addition of the diluent is beneficial for the mechanical properties studied and that the capacity of impact absorption obtained for the nanocomposites in this study is substantially greater than that for the other nanocomposites manufactured with CNTs that are described in the literature.

ACKNOWLEDGMENTS

The authors acknowledge the support provided by Petrobras for this research. Wellington M. Silva thanks the Brazilian agency CNPq (Conselho Nacional de Desenvolvimento Científico e Tecnológico) for financial support. The authors would like to thank the Instituto Nacional de Ciência e Tecnologia em Nanomateriais de Carbono—INCT, Centro de Microscopia—UFMG and to the Centro Federal de Educação Tecnológica of Minas Gerais—CEFET-MG. The authors also thank Prof. Hállen D.R. Calado for fruitful discussions.

REFERENCES

1. Oberlin, A.; Endo, M.; Koyama, T. *J. Cryst. Growth* **1976**, *32*, 335.
2. Iijima, S. *Nature* **1991**, *354*, 56.
3. Baughman, R. H.; Zakhidov, A. A.; de Heer, W. A. *Science* **2002**, *297*, 787.
4. Endo, M.; Strano, M. S.; Ajayan, P. M. In Carbon Nanotubes; Jorio, A.; Dresselhaus, M. S., Eds.; Springer: Berlin Heidelberg, **2008**, Vol. *111*, Chapter 2, pp 13.
5. De Volder, M. F.; Tawfick, S. H.; Baughman, R. H.; Hart, A. *J. Science* **2013**, *339*, 535.
6. Li, F.; Cheng, H. M.; Bai, S.; Su, G.; Dresselhaus, M. S. *Appl. Phys. Lett.* **2000**, *77*, 3161.
7. Yu, M. F.; Lourie, O.; Dyer, M. J.; Moloni, K.; Kelly, T. F.; Ruoff, R. S. *Science* **2000**, *287*, 637.
8. Berber, S.; Kwon, Y. K.; Tomanek, D. *Phys. Rev. Lett.* **2000**, *84*, 4613.
9. Terrones, M. *Int. Mater. Rev.* **2004**, *49*, 325.
10. Coleman, J. N.; Khan, U.; Blau, W. J.; Gun'ko, Y. K. *Carbon* **2006**, *44*, 1624.
11. Ma, P. C.; Siddiqui, N. A.; Marom, G.; Kim, J. K. *Compos. Part A* **2010**, *41*, 1345.
12. Ajayan, P. M.; Stephan, O.; Colliex, C.; Trauth, D. *Science* **1994**, *265*, 1212.
13. Tasis, D.; Tagmatarchis, N.; Bianco, A.; Prato, M. *Chem. Rev.* **2006**, *106*, 1105.
14. Datsyuk, V.; Kalyva, M.; Papagelis, K.; Parthenios, J.; Tasis, D.; Siokou, A.; Kallitsis, I.; Galiotis, C. *Carbon* **2008**, *46*, 833.
15. Bose, S.; Khare, R. A.; Moldenaers, P. *Polymer* **2010**, *51*, 975.
16. Sulong, A. B.; Park, J.; Lee, N.; Goak, J. *J. Compos. Mater.* **2006**, *40*, 1947.
17. Chen, Z.; Dai, X. J.; Magniez, K.; Lamb, P. R.; Rubin de Celis Leal, D.; Fox, B. L.; Wang, X. *Compos. Part A* **2013**, *45*, 145.
18. Sydlik, S. A.; Lee, J. H.; Walish, J. J.; Thomas, E. L.; Swager, T. M. *Carbon* **2013**, *59*, 109.
19. Silva, W. M.; Ribeiro, H.; Neves, J. C.; Calado, H. D. R.; Garcia, F. G.; Silva, G. G. *J. Therm. Anal. Calorim.* **2014**, *115*, 1021.
20. Wang, J.; Fang, Z.; Gu, A.; Xu, L.; Fu., L. *J. Appl. Polym. Sci.* **2006**, *100*, 97.
21. Guo, P.; Chen, X.; Gao, X.; Song, H.; Shen, H. *Compos. Sci. Technol.* **2007**, *67*, 3331.
22. Montazeri, A.; Javadpour, J.; Khavandi, A.; Tcharkhtchi, A.; Mohajeri, A. *Mater. Des.* **2010**, *31*, 4202.
23. Montazeri, A.; Montazeri, N. *Mater. Des.* **2011**, *32*, 2301.
24. Hadavand, B. S.; Javid, K. M.; Gharagozlou, M. *Mater. Des.* **2013**, *50*, 62.
25. Singh, S.; Srivastava, V. K.; Prakash, R. *Mater. Sci. Technol.* **2013**, *29*, 1130.
26. Spitalsky, Z.; Tasis, D.; Papagelis, K.; Galiotis, C. *Prog. Polym. Sci.* **2010**, *35*, 357.
27. Cui, L. J.; Wang, Y. B.; Xiu, W. J.; Wang, W. Y.; Xu, L. H.; Xu, X. B.; Meng, Y.; Li, L. Y.; Gao, J.; Chen, L. T.; Geng, H. Z. *Mater. Des.* **2013**, *49*, 279.
28. Yang, K.; Gu, M.; Guo, Y.; Pan, X.; Mu, G. *Carbon* **2009**, *47*, 1723.
29. Ye, Y.; Chen, H.; Wu, J.; Ye, L. *Polymer* **2007**, *48*, 6426.
30. Sun, L.; Gibson, R. F.; Gordaninejad, F.; Suhr, J. *Compos. Sci. Technol.* **2009**, *69*, 2392.

31. Chen, Z. K.; Yang, G.; Yang, J. P.; Fu, S. Y.; Ye, L.; Huang, Y. G. *Polymer* **2009**, *50*, 1316.
32. Bakar, M.; Szymanska, J.; Rudecka, J.; Fitas, J. *Polym. Polym. Compos.* **2010**, *18*, 503.
33. Rahman, M. M.; Hosur, M.; Zainuddin, S.; Jajam, K. C.; Tippur, H. V.; Jeelani, S. *Polym. Test.* **2012**, *31*, 1083.
34. Yi, X. F.; Mishra, A. K.; Kim, N. H.; Ku, B. C.; Lee, J. H. *Compos. Part A* **2013**, *49*, 58.
35. Putz, K. W.; Palmeri, M. J.; Cohn, R. B.; Andrews, R.; Brinson, L. C. *Macromolecules* **2008**, *41*, 6752.
36. Ribeiro, H.; Silva, W. M.; Neves, J. C.; Calado, H. D. R.; Paniago, R.; Seara, L. M.; Camarano, D. M.; Silva, G. G. *Polym. Test.* **2015**, *43*, 182.
37. Economopoulos, S. P.; Karousis, N.; Rotas, G.; Pagona, G.; Tagmatarchis, N. *Curr. Org. Chem.* **2011**, *15*, 1121.
38. Garcia, F. G.; Soares, B. G.; Pita, V. J. R. R.; Sánchez, R.; Rieumont, J. *J. Appl. Polym. Sci.* **2007**, *106*, 2047.
39. Trigueiro, J. P. C.; Silva, G. G.; Lavall, R. L.; Furtado, C. A.; Oliveira, S.; Ferlauto, A. S.; Lacerda, R. G.; Ladeira, L. O.; Liu, J. W.; Frost, R. L.; George, G. A. *J. Nanosci. Nanotechnol.* **2007**, *7*, 3477.
40. Murphy, H.; Papakonstantinou, P.; Okpalugo, T. T. *J. Vac. Sci. Technol., B* **2006**, *24*, 715.
41. Vuković, G.; Marinković, A.; Obradović, M.; Radmilović, V.; Čolić, M.; Aleksić, R.; Uskoković, P. S. *Appl. Surf. Sci.* **2009**, *255*, 8067.
42. Silva, W. M.; Ribeiro, H.; Seara, L. M.; Calado, H. D. R.; Ferlauto, A. S.; Paniago, R. M.; Leite, C. F.; Silva, G. G. *J. Braz. Chem. Soc.* **2012**, *23*, 10781086.
43. Yang, D. Q.; Rochette, J. F.; Sacher, E. *Langmuir* **2005**, *21*, 8539.
44. Xia, W.; Wang, Y.; Bergsträßer, R.; Kundu, S.; Muhler, M. *Appl. Surf. Sci.* **2007**, *254*, 247.
45. Zhang, G.; Sun, S.; Yang, D.; Dodelet, J. P.; Sacher, E. *Carbon* **2008**, *46*, 196.
46. Ribeiro, H.; Silva, W. M.; Rodrigues, M. T. F.; Neves, J. C.; Paniago, R. M.; Leite, C. F.; Calado, H. D. R.; Seara, L. M.; Silva, G. G. *J. Mater. Sci.* **2013**, *48*, 7883.
47. Gojny, F. H.; Wichmann, M. H.; Fiedler, B.; Schulte, K. *Compos. Sci. Technol.* **2005**, *65*, 2300.
48. Ayatollahi, M. R.; Shadlou, S.; Shokrieh, M. M. *Eng. Fract. Mech.* **2011**, *78*, 2620.
49. Moaseri, E.; Karimi, M.; Baniadam, M.; Maghrebi, M. *Compos. Part A* **2014**, *64*, 228.
50. Thostenson, E. T.; Chou, T. W. *Carbon* **2006**, *44*, 3022.
51. Hosur, M.; Barua, R.; Zainuddin, S.; Kumar, A.; Trovillion, J.; Jeelani, S. *J. Appl. Polym. Sci.* **2013**, *127*, 4211.
52. Isik, I.; Yilmazer, U.; Bayram, G. *Polymer* **2003**, *44*, 6371.
53. Miyagawa, H.; Drzal, L. T. *Polymer* **2004**, *45*, 5163.
54. Jyotishkumar, P.; Logakis, E.; George, S. M.; Pionteck, J.; Häussler, L.; Haßler, R.; Pissis, P.; Thomas, S. *J. Appl. Polym. Sci.* **2013**, *127*, 3063.
55. Jajam, K. C.; Rahman, M. M.; Hosur, M. V.; Tippur, H. V. *Compos. Part A* **2014**, *59*, 57.
56. Korayem, A. H.; Barati, M. R.; Simon, G. P.; Zhao, X. L.; Duan, W. H. *Compos. Part A* **2014**, *61*, 126.